

AGN Clustering and Environments in X-ray Surveys

A review

Takamitsu Miyaji

**Department of Physics
Carnegie Mellon University**

Extragalactic Surveys
A Chandra Science Workshop
November, 2006

Scope of the Talk

1. Large Scale Structure in X-ray AGNs: Intro
2. Two point Correlation Function Measurements from X-ray data: Basics and Practice
3. Summary of Correlation Function results from various surveys
4. Some Cosmological Implications
5. Other approaches
6. Summary

1. Large Scale Structure in X-ray Surveys: Introduction

No. 1, 1990

X-RAY FLUX DIPOLE OF AGNs

L5

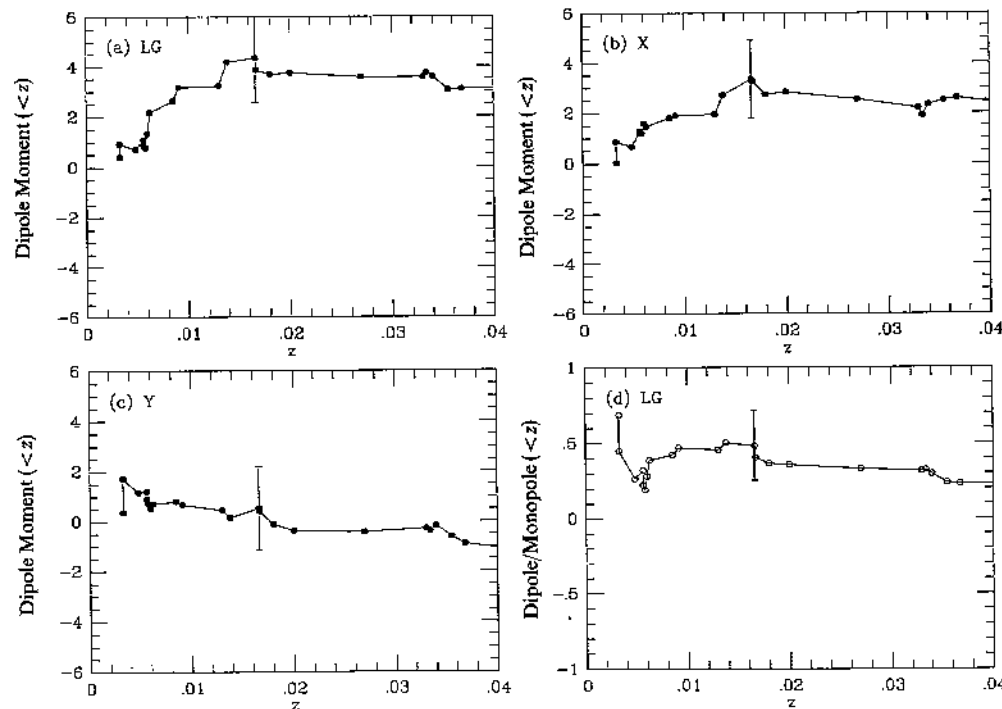


FIG. 2.—Dipole growth curves (eq. [1]) for the components in three orthogonal directions are shown in (a)–(c). Fig. 2d shows growth curve of the ratio of dipole/monopole (eq. [2]) for LG direction. Error bars show statistical sampling errors.

Miyaji & Boldt 1990

- Matter in the universe has a structure. Galaxies, AGNs, Clusters of galaxies etc. trace the underlying structure in mass.

- Clustering properties of AGNs provide yet another clue to understanding the formation and evolution of Supermassive Blackholes (SMBH).
- Simple characterization of how AGNs trace underlying mass: bias parameter

$$b_{\text{AGN}} = (\delta\rho / \langle\rho\rangle)_{\text{AGN}} / (\delta\rho / \langle\rho\rangle)_{\text{mass}}$$

(contrast enhancement factor)

- Bias $b > 1$ when a tracer samples high tips of underlying mass density (Kaiser '84).
- Biasing of theoretical Dark Matter Halos (DMH) depends is mass dependent.

2. Two-point Correlation Function on X-ray data: Basics and Practice

- Excess number of pairs separated by r or θ over random distribution
- Joint probability δP of finding an object in both of the solid angle elements separated by r/θ is represented by:

$$\text{Angular: } \delta P = n^2 [1 + \underline{w(\theta)}] \delta \Omega_1 \delta \Omega_2, \quad \text{3D: } \delta P = n^2 [1 + \underline{\xi(r)}] \delta V_1 \delta V_2$$

- Two point 3-D correlation function is related to bias parameter by:

$$\xi_{\text{AGN}}(r) = b_{\text{AGN}}^2 \xi_{\text{mass}}(r)$$

- Estimators (DD, RD, and RR are *normalized* numbers of source-source, source-random and random-random pairs respectively):

$$\rightarrow w_{\text{est}}(\theta) = (DD/RD) - 1 \quad (\text{Efsthathiou} + 1991)$$

$$\rightarrow w_{\text{est}}(\theta) = (DD - RR) / (DR - DR) - 1 \quad (\text{Hamilton} 1993)$$

$$\rightarrow w_{\text{est}}(\theta) = (DD - 2RD - RR) / RR \quad (\text{Landy \& Szalay} 1996)$$

- They give basically the same results, with some different error properties.

Depending on the availability of redshift information

- **Angular Correlation function $w(\theta)$** , poor man's measure, signal diluted by projection effects. No redshift information, but redshift distribution can be modeled. Use Limber's equation to de-project to $\xi(r)$
- **Projected distance correlation function $w_p(r_p)$**
Redshift information, even photo-z. Use with redshift-divided samples to improve S/N.
- Correlation function in 2 parameter space (projected dist and redshift space) $\xi(r_p, \pi)$
- 3-D correlation function in redshift space $\xi(\mathbf{s})$ with $s^2 = r_p^2 + \pi^2$ used when spect-z's are available. Redshift distortion ...

Technicalities

- Error/Covariance Matrix Estimations
 - ➔ Poissonian of the number of pairs $(1+w)/\sqrt{DD}$ or full Poisson expression (fit with C-stat) if the number of pairs are small
 - ➔ Jackknife resampling (can create covariance matrix) (needs large number of independent regions)
 - ➔ Random Monte-Carlo scaled by $(1+w)$ (TM+, '07)
 - ➔ Monte-carlo using mock catalogs (including clustering)
- Integral constraint gives an offset to w for estimated in finite area. Correction is model dependent.

$$\iint w_{\text{est}} d^2\Omega = 0.$$

- Amplification bias (Vikhlinin & Forman '95) due to PSF smoothing: several percent effect for typical medium-depth XMM survey (Basilakos04,05; TM+ '07). Negligible in Chandra Surveys
- Random sample generation

Random Sample Generations

- Sensitivity varies over the field, possibly producing spurious clustering signal.
- This can be compensated by applying the same sensitivity cut to the random sample.

1. Full X-ray Image simulation and source detection

(Murray+'06, Gandhi+'06, TM+'07, Carrera+submitted)

Requires a Log N-Log S model/Computationally demanding.

2. The CR of the random source is drawn from an externally given Log N-Log S relation (Basilakos+'04, Pucetti+'06, Carrera+)

1. Good sensitivity map and Log N-Log S model.

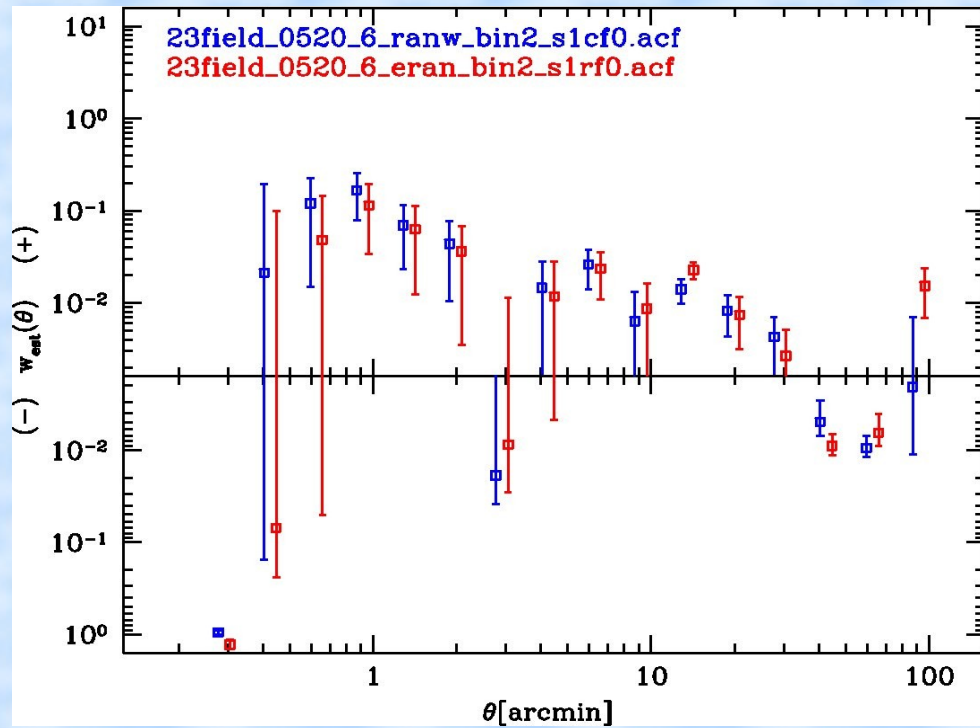
3. Take the Countrate (CR) distribution from actual sources (TM+'07)

Good sensitivity map. Good for, e.g., investigate subsamples.

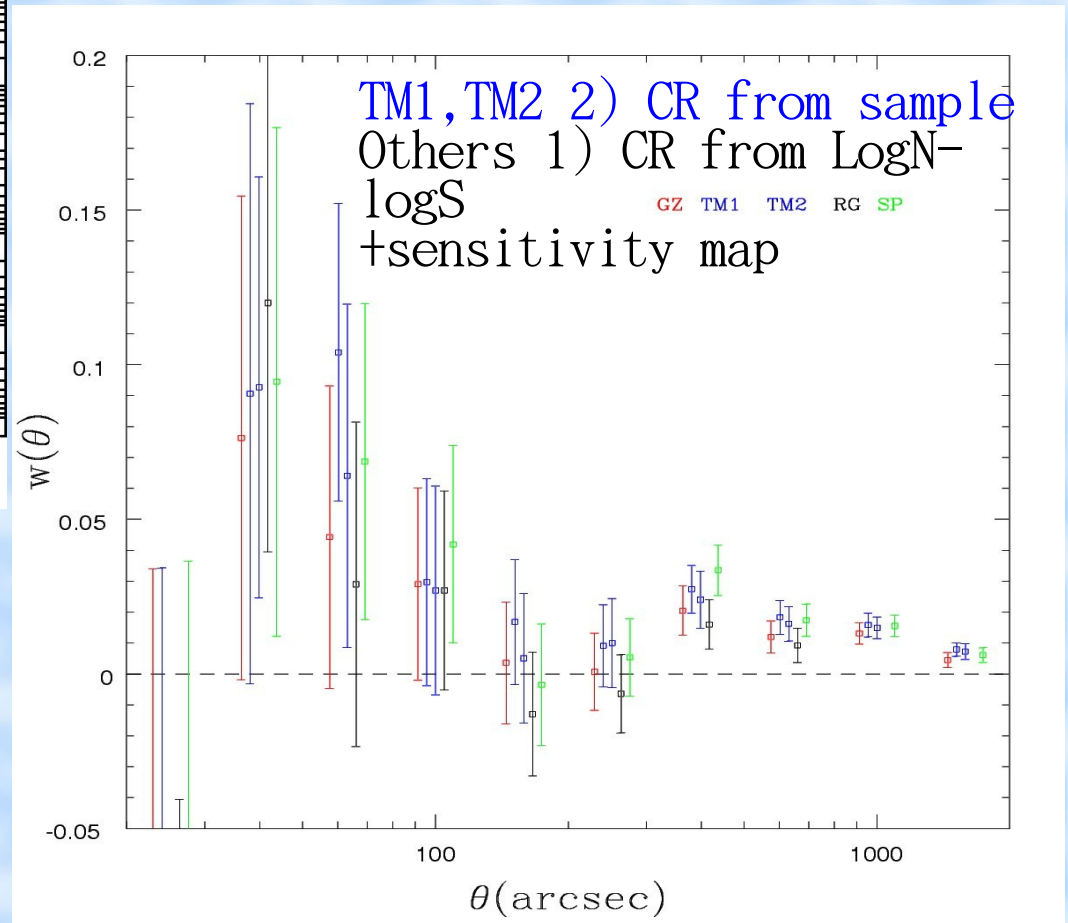
4. Make survey as uniform as possible by dense tiling (XMM-COSMOS year-2, C-COSMOS)

Comparing Random Sample Methods (XMM-COSMOS 23 field data)

Having a Good Sensitivity map and a good log N-log S model, different methods give consistent results.



2) CR from Sample+sensitivity map vs 3) Simulated random



Limber De-Projection to 3D-Correlation Function

The 2-D ACF is a projection of the real-space 3-D ACF of the sources ($\xi(r)$) along the line of sight. The relation is expressed by the Limber's equation:

$$w(\theta)N^2 = \int \left(\frac{dN}{dz}\right)^2 \int \xi(\sqrt{[d_A(z)\theta]^2 + l^2}) (dz/dl) dl dz,$$

where $d_A(z)$ is the angular distance at the redshift z , N is the total number of sources and dN/dz is the redshift distribution (per z) of the sources. The redshift evolution of the 3-D correlation function is customarily expressed by:

$$\xi(r, z) = (r/r_0)^{-\gamma} (1+z)^{-3-\epsilon}$$

Clustering evolution

In the above expression, $\epsilon = -3$ corresponds to the case where the correlation length is constant in the physical coordinates and $\epsilon = \gamma - 3$ corresponds to the case the clustering is constant in the comoving coordinates.

The relationship between zero-redshift 3-D correlation length r_0 and the 2-D correlation length θ_c is then:

$$r_0^\gamma = (N^2/S) \theta_c^{\gamma-1},$$

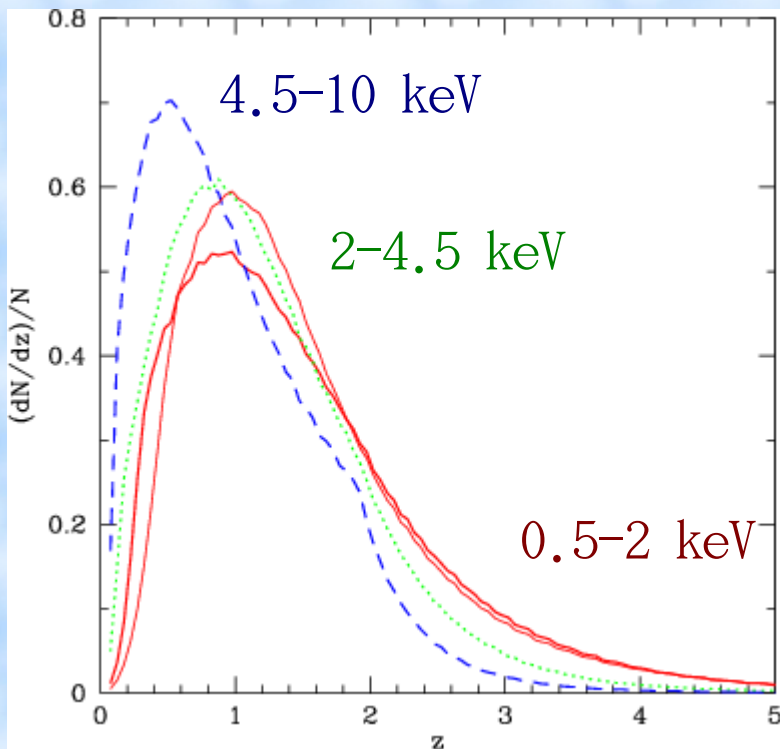
$$S = H_\gamma \int \left(\frac{dN}{dz}\right)^2 \left(\frac{cd\tau(z)}{dz}\right)^{-1} d_A^{1-\gamma} (1+z)^{-3-\epsilon} dz$$

$$H_\gamma = \frac{\Gamma[(\gamma-1)/2]\Gamma(1/2)}{\Gamma(\gamma/2)},$$

where $\tau(z)$ is the look back time. All dependences on cosmological parameters are included in $d_A(z)$ and $\tau(z)$.

Model Redshift Distribution

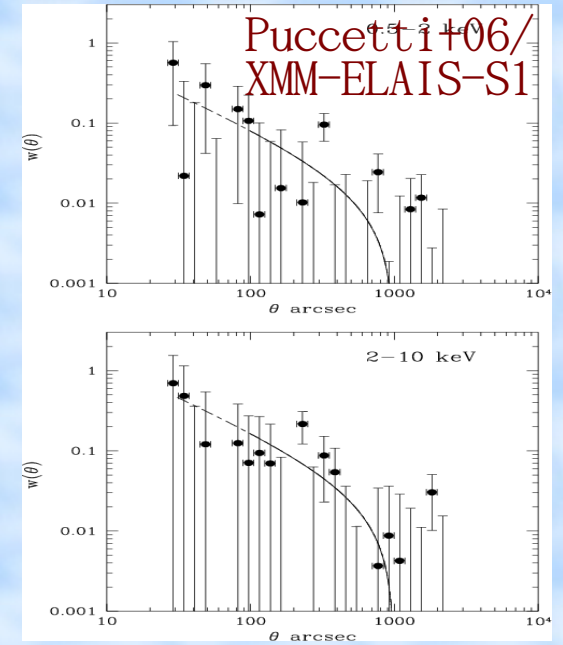
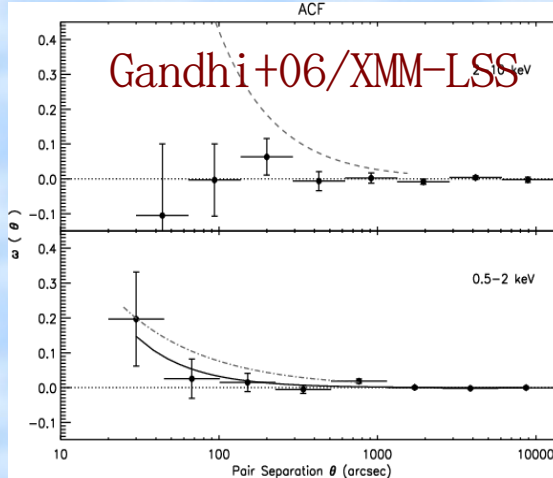
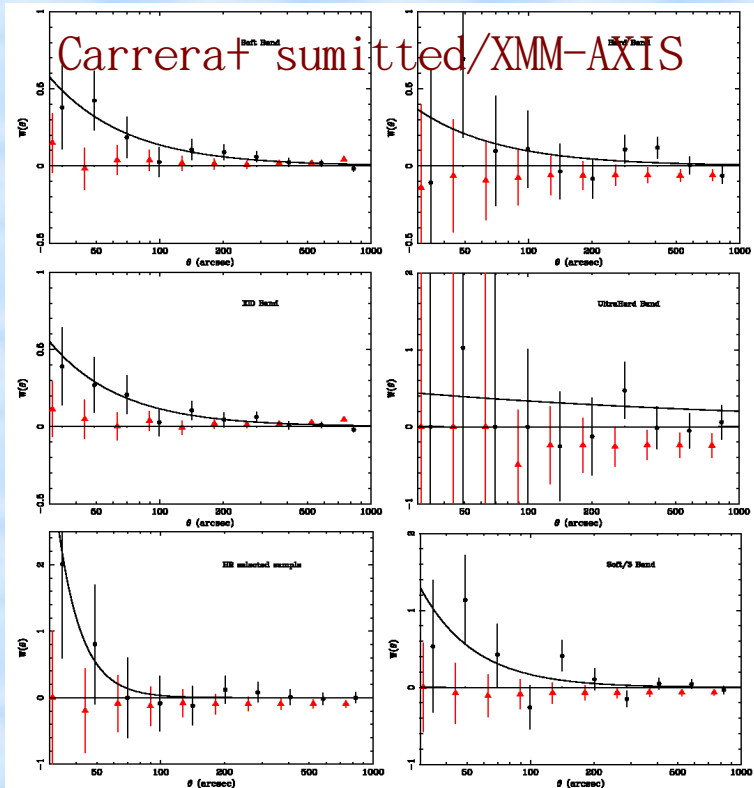
For de-projection of the angular ACF/CCF, we need the redshift distribution of the sources.



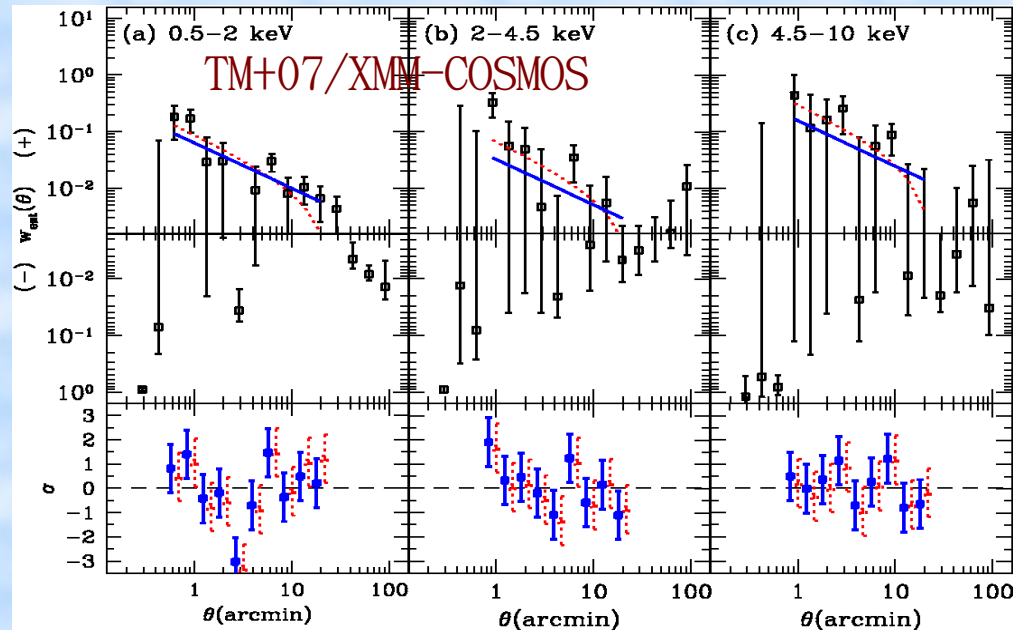
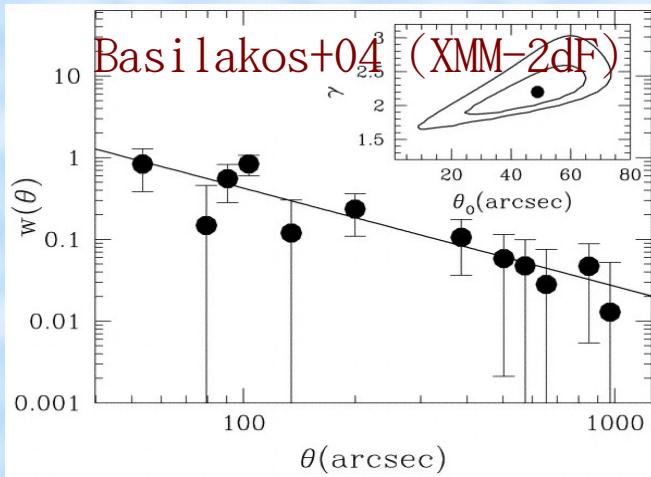
Redshift distributions of the XMM-COSMOS X-ray sources detected in the three bands used in the de-projection, calculated using Ueda et al. (2003, ApJ 598, 886;U03) model except the thin red solid line, which is from Hasinger, Miyaji, Schmidt (2005, A&A 441, 417;H05)

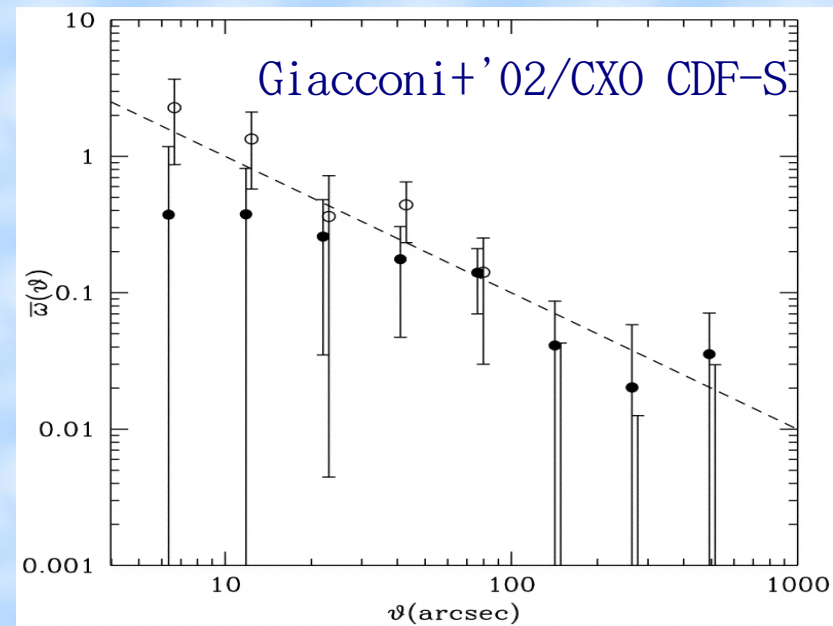
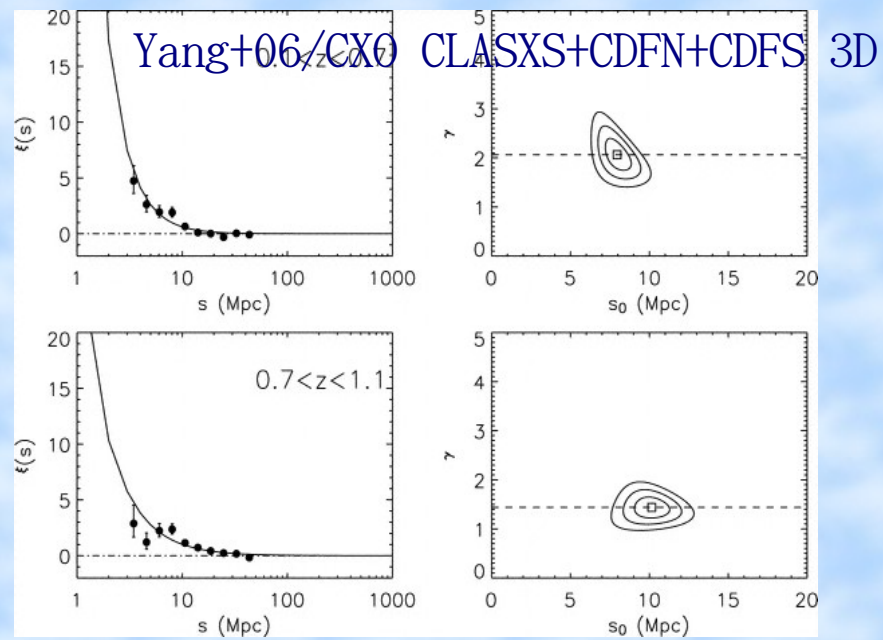
From TM+ '07 for XMM-COSMOS

3. AGN/QSO Correlation Function Measurements and Comparisons

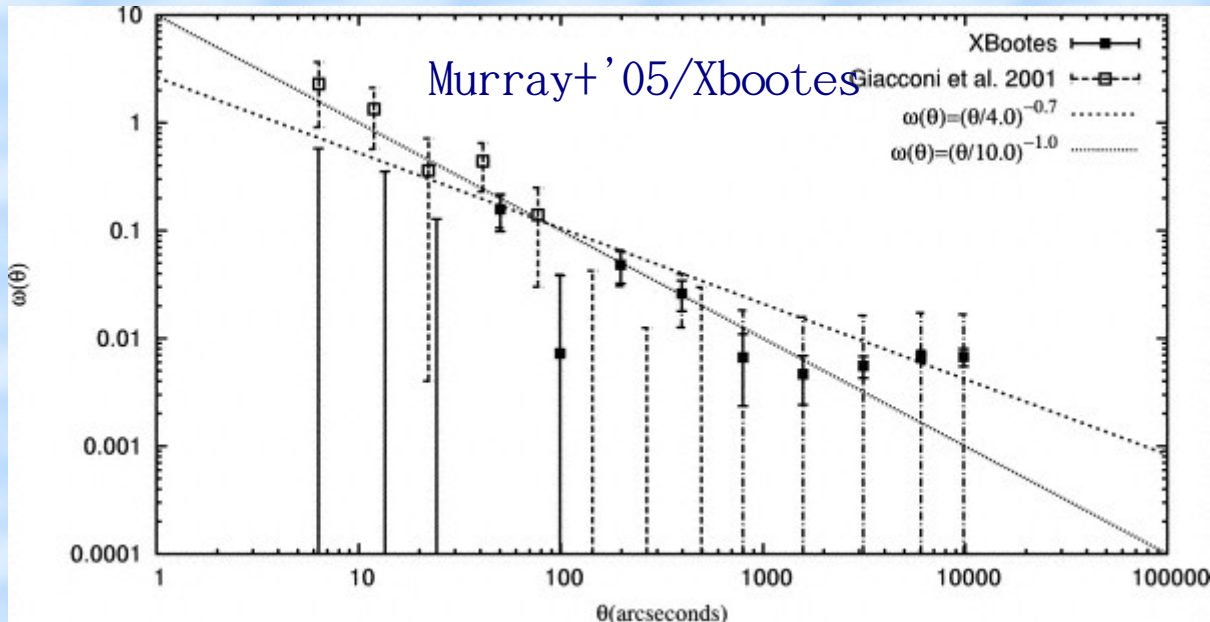
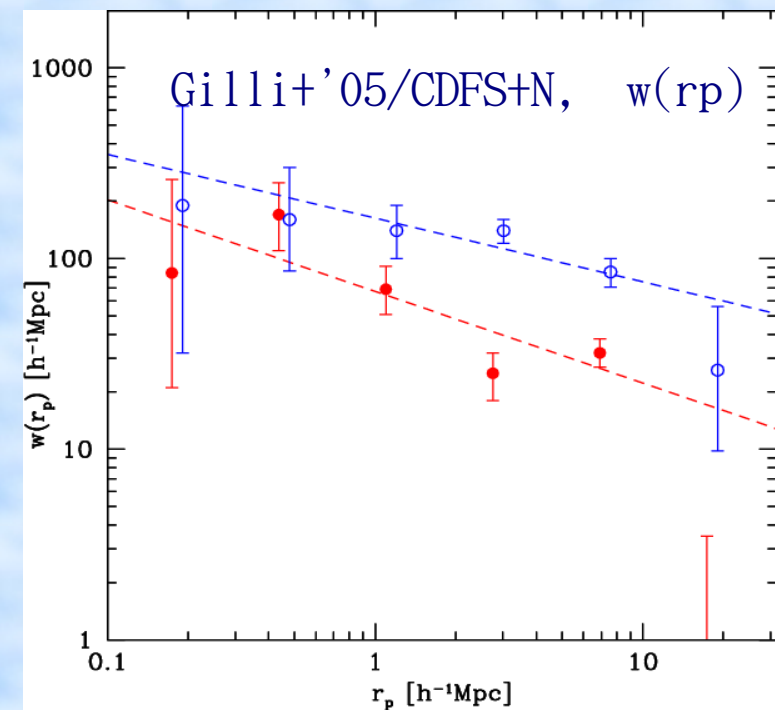


XMM-NEWTON





Chandra



Summary of Correlation Lengths

Survey	Band	N_{src}	$\langle z \rangle$	Method	γ	$r_0/s_0 \ h^{-1} \text{Mpc}$	Ref
RASS	0.1-2.4 keV	2096	0.15	$w(\theta)$	1.8*	6.5 ± 1.0	Akylas+'00
AERQS	0.1-2.4 keV	392 w/z	0.06	$\xi(s)$	1.56	8.6 ± 2.0	Grazian+'04
RASS-NEPS	0.1-2.4 keV	219 w/z	0.22	$\xi(s)$	1.8*	7.4 ± 1.8	Mullis+'04
XMM-2dF	0.5-2 keV	432	1.19	$w(\theta)$	1.8*	16.4 ± 1.3	Basilakost,'05
"	2-10 keV	171	0.75	"	1.8*	19.0 ± 3.0	Basilakost,'04
XMM-COSMOS	0.5-2 keV	1037	1.07	"	1.8*	9.4 ± 0.8	TM+'07
"	2-4.5 keV	545	0.87	"	1.8*	$6.9(+2.2;-3.1)$	"
"	4.5-10 keV	151	0.60	"	1.8*	$12.7(+2.3;-2.7)$	"
XMM-ELAIS S1	0.5-2 keV	395	1.00	"	1.8*	12.8 ± 4.2	Puccetti+'06
"	2-10 keV	205	0.85	"	1.8*	17.9 ± 4.8	"
CXO-CLASXS+CDF	2-8 keV	168 w/z	0.45	$\xi(s)$	1.9 ± 0.3	7.9 ± 0.9	Yang+'06
"	"	151 w/z	0.92	"	1.4 ± 0.2	$10.1(+1.1;-1.0)$	
"	"	77 w/z	1.26	"	2.0 ± 0.7	$8.4(+1.8;-2.4)$	"
"	"	89 w/z	2.07	"	1.7 ± 0.5	$12.4(+2.7;-3.4)$	"
CXO-CDFS	0.5-10 keV	97 w/z	0.84	$w_p(r_p)$	1.33 ± 0.14	10.3 ± 1.7	Gilli+'05
CXO-CDFN	"	160 w/z	0.96	"	1.50 ± 0.12	5.5 ± 0.6	"

- $\xi(r) = (r/r_0)^{-\gamma}$ (real-space) or $\xi(s) = (s/s_0)^{-\gamma}$ (redshift-space),
- comoving coordinates
- Assuming clustering evolution fixed in comoving coord.

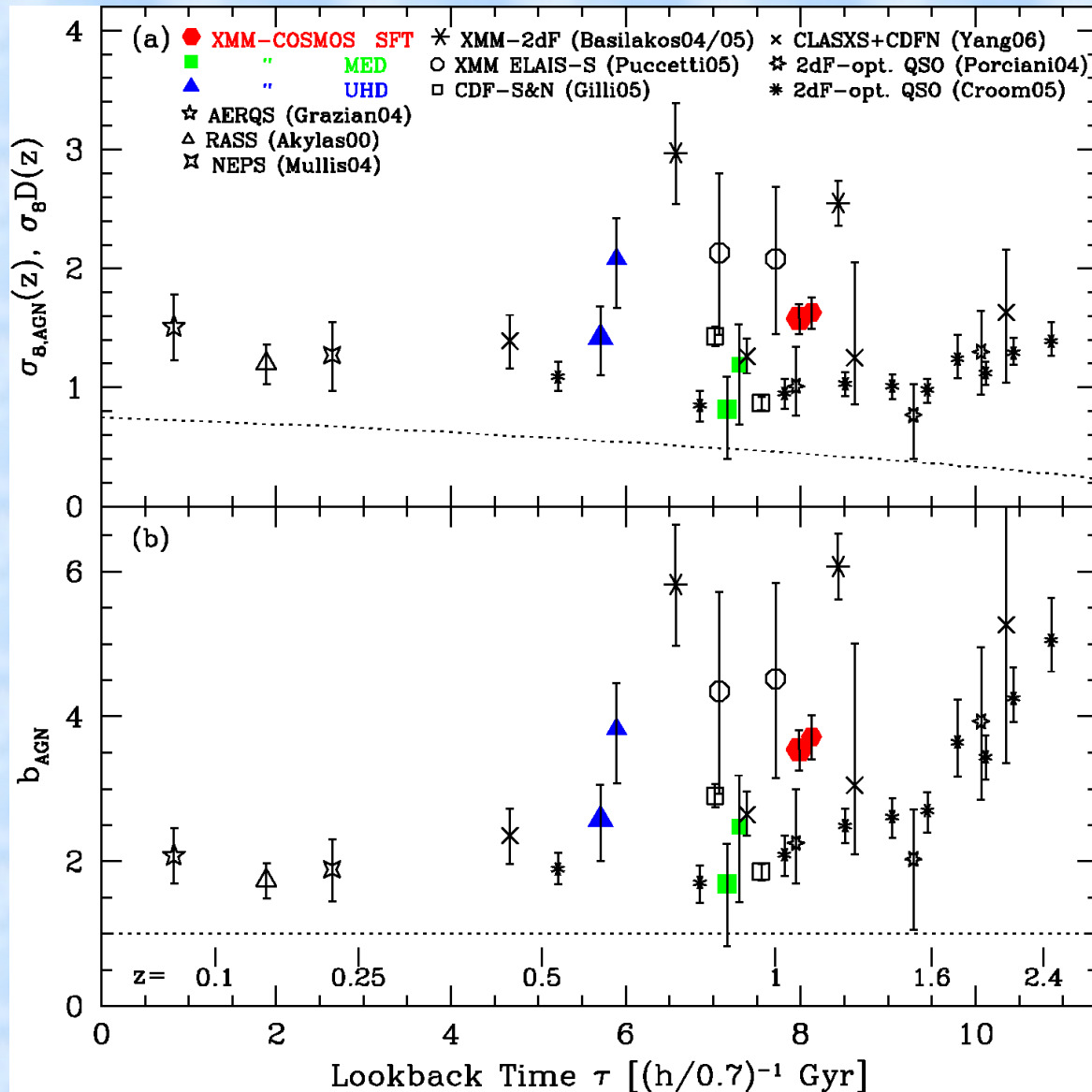
Comparison with Other work and Bias Parameters of AGN clustering (TM+07 approach)

- Convert the 3-D correlation functions to the RMS density fluctuations in $8h^{-1} \text{ Mpc}^{-1}$: $\sigma_{8,\text{AGN}}(z)$

$$\sigma_{8,\text{AGN}}^2 = \int \int \xi(|\mathbf{r}_1 - \mathbf{r}_2|) dV_1 dV_2 / V^2$$

- Direct comparison with DM fluctuation: $\sigma_8 D(z)$.
- Insensitive to assumed slope, when γ is fixed.
- Convert AGN/QSO ACF measurements from literature to the same $\sigma_{8,\text{AGN}}(z)$.
- Plot against the effective mean redshift of the sample from various works.

Density Fluctuation and Bias



- Convert $\xi(r, z)$ to $\sigma_{8,AGN}(z)$: the rms fluctuation in the $8h^{-1}$ Mpc sphere. Comparison on the common ground.
- Comparison with $\sigma_8 D(z)$ mass distribution from the linear theory with WMAP σ_8 .
- Bias parameter of the X-ray AGN distribution $b_{AGN} = \sigma_{8,AGN}(z) / \sigma_8 D(z)$

Trends

- No evidence for difference between obscured and unobscured AGNs (by X-ray colors) (directly by Gilli+ '05, Yang+ '06, indirectly by some XMM $w(\theta)$'s)
- CDF-S has stronger clustering amplitude ($\approx \times 1.6$) than HDF/CDF-N (Gilli+ '05).. Cosmic Variance
- A weak dependence of clustering amplitude with L_x (Yang + '06)

4. Some Cosmological Implications

Typical Mass of Dark Matter Halo that these AGNs reside

- Typical Mass of the Dark Matter Halo is a function of bias parameter (e.g. Mo & White 1996; Sheth, Mo, Tormen 2001)

$$b(M, z) = 1 + \frac{1}{\sqrt{a}\delta_c(z)} \left[av^2\sqrt{a} + 0.5\sqrt{a}(av^2)^{(1-c)} - \frac{(av^2)^c}{(av^2)^c + 0.5(1-c)(1-c/2)} \right]$$

- For XMM-AGNs along with some CXO AGNs in literature:

Sheth, Mo, Tormen 2001

$$b_{\text{AGN}} \approx 2-4, M_{\text{halo}} \approx 10^{13}-10^{14} M_{\odot}$$

$$n(> \sim M_{\text{halo}}) \approx 10^{-3}-10^{-4} h^{-1} \text{Mpc}^{-3} \quad (\text{Halo MF by Jenkins+2001, Warren+2006})$$

This is 1-10 times the number density of AGNs (unobscured+obscured) ($\log L_x > \approx 42.5$ at $z \approx 1$) approximately represented by the sample.

cf. Luminous Optical QSOs: $M_{\text{halo}} = \text{a few } \times 10^{12} M_{\odot}$ (e.g. Croom+05,)

Lifetime of AGN activity

Lifetime of QSO activity t_Q (Martini & Weinberg 01; Haimann & Hui 01) can be estimated assuming....

1. At most one active QSO at a time in a halo.
2. QSO luminosities are associated with halo mass monotonically
3. The existence of SMBH is the only requirement for QSO activity

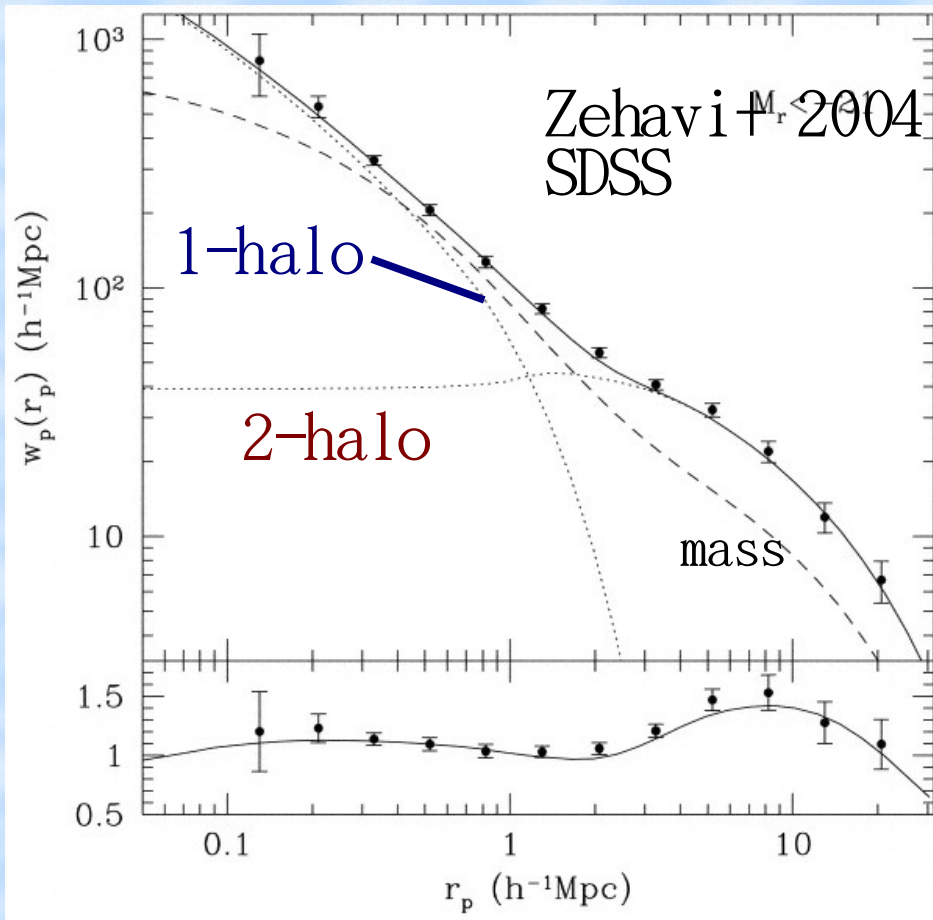
$$\text{QSO Bias} \rightarrow \langle M_{\text{halo}} \rangle$$
$$\text{Duty cycle} \approx n(>L_{\text{QSO},\text{min}}) / n(>M_{\text{halo},\text{min}}) \approx t_Q / t_{\text{halo}}$$

- Works for luminous QSOs, (e.g Croom+05, $t_Q \approx 10^7 \text{yr}$)
- Crudely for XMM-Newton X-ray AGNs at $z \approx 1$, $\log L_x \approx 42.5$,
 $n \approx \text{a few} \times 10^{-4} \text{ h}^{-1} \text{ Mpc}^{-3}$, duty cycle $\approx 0.1-1$
- At $0.8 < z < 2$, $t_{\text{AGN}} \approx \text{Gyr}$
- Some of the above assumptions are not valid. (A single halo contains multiple galaxies and each of them has a SMBH)

Current popular halo model for galaxies

- Two point Correlation Function=

1-halo term+2-halo term



- Fit with Halo Occupation Model $N_{\text{gal}}(M_{\text{halo}})$ (Cooray & Sheth '02 for review)
- For local SDSS galaxies, more than one galaxy per halo for $M_{\text{halo}} > \text{a few } \times 10^{-12} M_{\odot}$
- A similar result at $0.4 < z < 0.8$ (e.g. Phelps+ '06/Combo-17)
- Apply to X-ray AGN to galaxy Cross-correlation?

Further Cosmological Implications?

COSMOLOGICAL PARAMETERS FROM THE LIKELIHOOD ANALYSIS					
Data	Ω_m	w	σ_8	b_0	χ^2/dof
<i>XMM-Newton</i>	0.28 ± 0.03	$w = -1$	0.75 ± 0.03	$2.0^{+0.20}_{-0.25}$	0.90
<i>XMM-Newton/SN Ia</i>	0.26 ± 0.04	$-0.90^{+0.10}_{-0.05}$	0.73	2.0	0.87

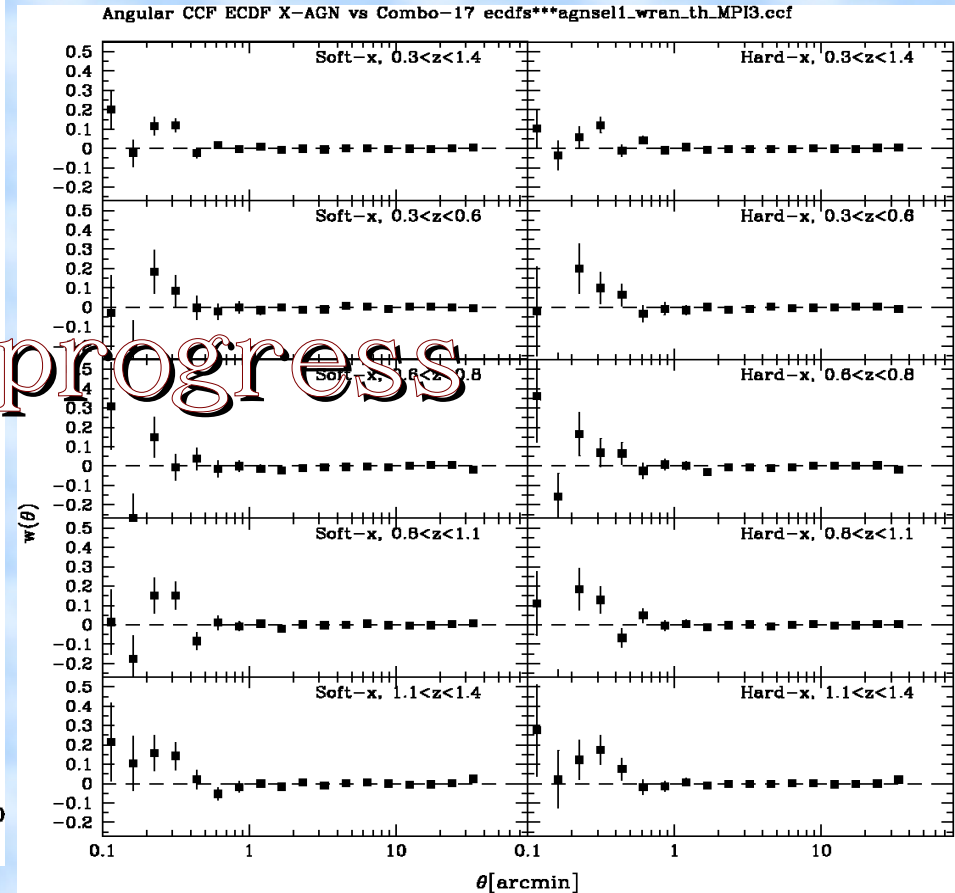
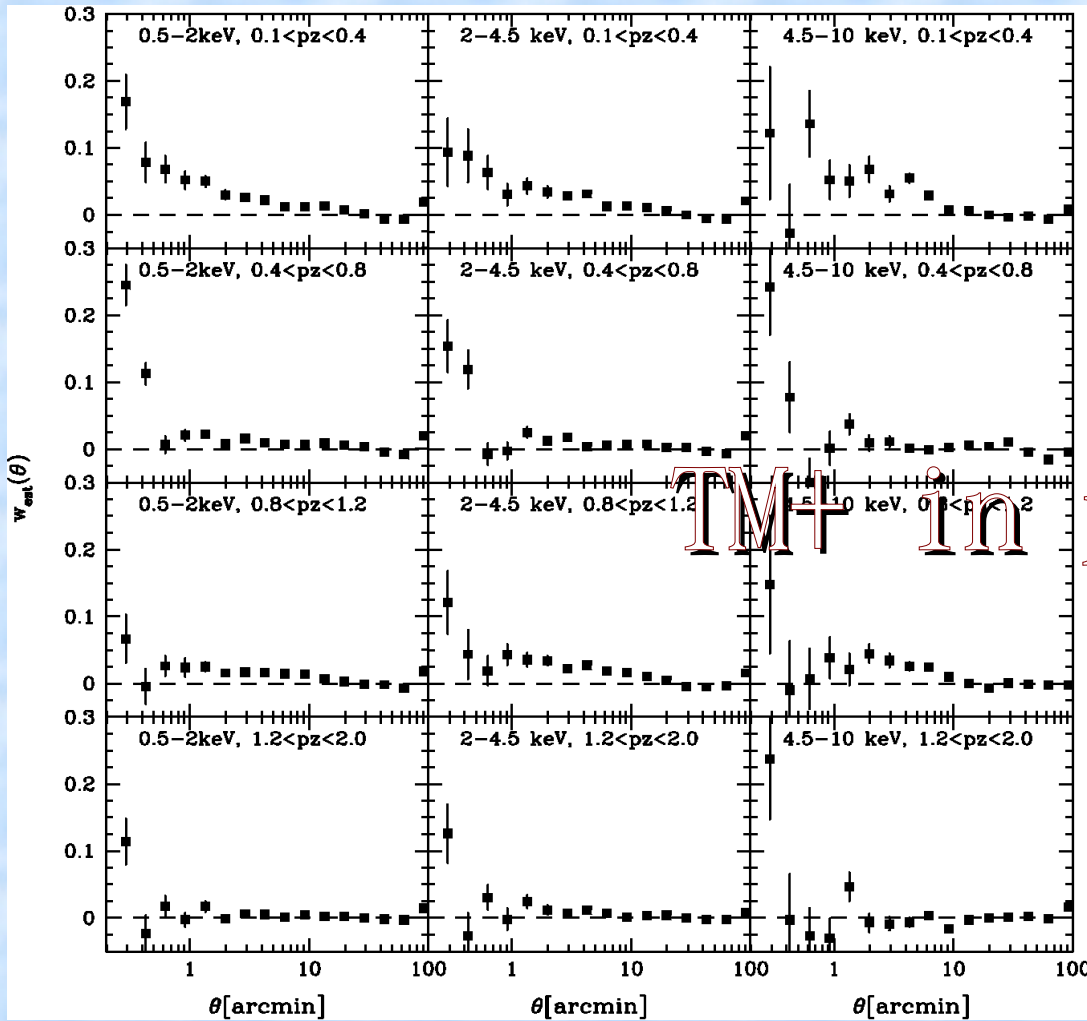
Basilakos & Plionis 2006

- Basilakos & Plionis (2005, 2006) went further by fitting $w_{\text{AGN}}(\theta)$ with a model involving cosmological parameters assuming:
 - Linear biasing ($b(z)$) is scale independent. here is a redshift dependence.
 - AGN bias at $z=0$ (b_0) is a free parameter of fit.
 - Dependence of cosmology is solely in slope/shape of ACF
 - Sensitivity of the results to linear biasing assumption?
 - In excellent agreement with the WMAP results!

5. Other Approaches

- Cross-correlation function with other classes of objects:
 - $\xi_{\text{agn-gal}} = b_{\text{agn}} b_{\text{gal}} \xi_{\text{mass}}$
 - **With clusters:**
 - Cappelluti+’05 in cluster fields, +’07 in NEPS.
 - **With galaxies** (better statistics for precise investigations, also traces more local environments):
 - TM+ in XMM-COSMOS/E-CDFS
 - Coil+ in EGS (this session)
 - Francket+ poster
 - Ly-break gal vs X-ray src $b_{\text{AGN}} \approx 6 @ z=3$
 - See also Cheng, Kauffmann+’06 (SDSS NLAGN+Galaxies)

Galaxies vs X-ray Source



TMT in progress

XMM-COSMOS vs Galaxies

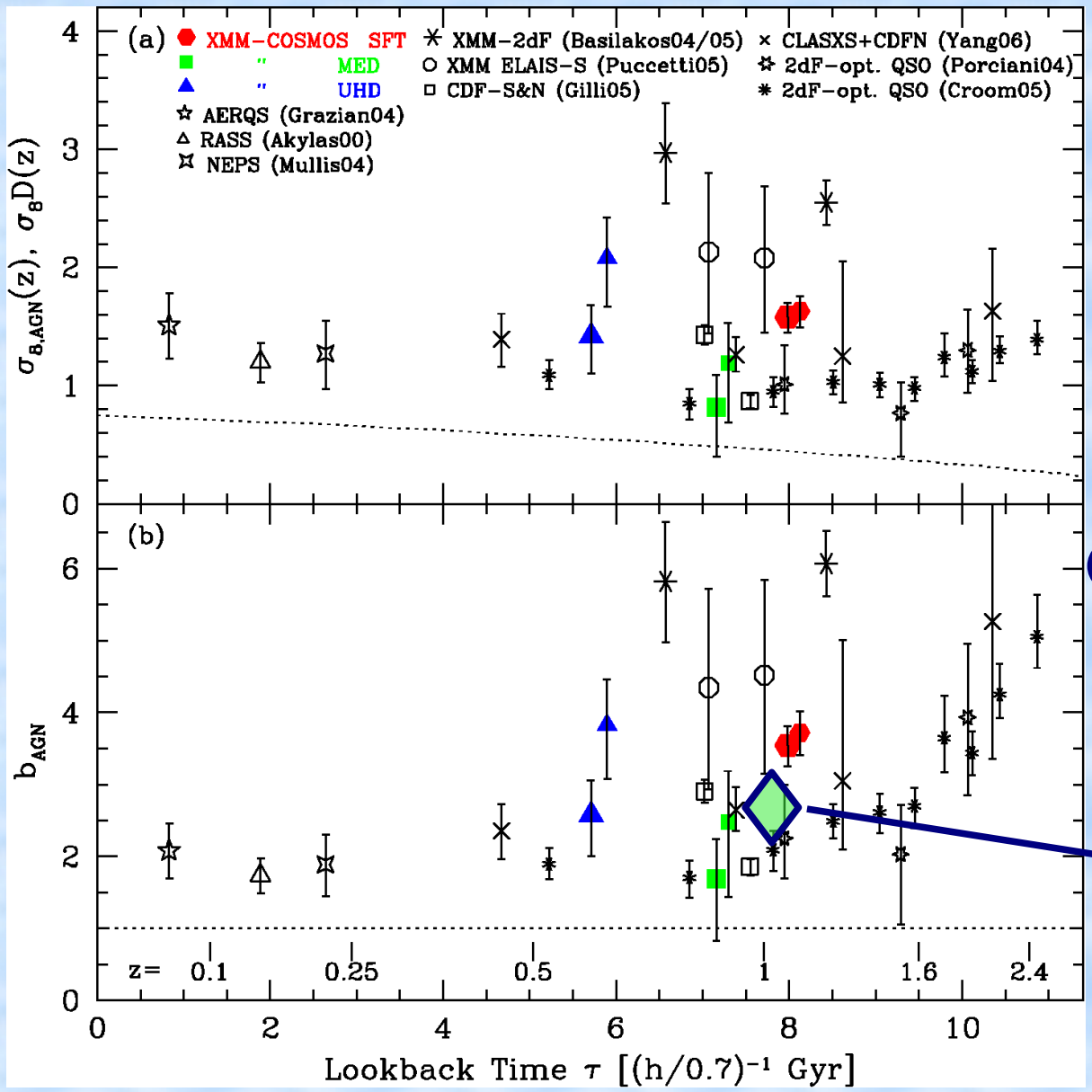
ECDFS AGN vs Combo-17 galaxies

- **Excess Variance**

- Yang+ '03, LHNW (CLASXS): **hard band sources are more strongly clustered, but see their own recent $\xi(s)$ studies...**
- Stewart, poster: 2XMM catalog. 16% of excess variance for $S_x > 1e-14$ cgs, **$b_{AGN} \approx 2.6$ @ $z \approx 1-2$.**

- **Galaxy counts around X-ray AGNs and comparison with environments of non-AGN galaxies**

- 31 AGNs in $0.4 < z < 0.6$ have the same local environment (< 500 kpc) as galaxies with similar morphologies. Minor merger for fueling (Waskett+ 06)?
- 53 X-ray AGNs at $z \approx 1$ avoid underdense regions. AGN with blue host reside in denser environment than galaxies in AEGIS (Georgakakis+ '06)



○ Francke, CCF with Ly-break

◇ Stewart Excess Variance

Summary

- Current status of correlation function and environmental studies in X-ray surveys are reviewed.
- Technical aspects of two-point correlation functions are discussed
- $b_{\text{AGN}} \approx 2$ in local universe, $b_{\text{AGN}} \approx 2-6$ at $z > 1$
- The b_{AGN} values of AGNs at $z \approx 1$ suggest associations with $10^{13}-10^{14} M_{\odot}$ dark matter halos.
- Cross-correlation with galaxies and galaxy counts around AGNs are starting to give clues to local environment, leading to the understanding of fueling mechanism.